

# Modeling pulsed nonlinear ultrasound for medical applications: the INCS method

M.D. Verweij, J. Huijssen

*Laboratory of Electromagnetic Research, Delft University of Technology, Delft, The Netherlands,*

*Email: m.d.verweij@tudelft.nl*

## Introduction

The higher harmonics in nonlinear ultrasound fields are known to yield opportunities for improving the image quality of medical echoscopy. For this purpose, the optimization of medical imaging devices and techniques requires the accurate simulation of nonlinear ultrasound fields in tissue. A successful simulation method should be able to compute the pulsed ultrasound field of a phased array transducer in a nonlinear and attenuating medium. Moreover, the method should cope with a large-scale domain (approximately 100 wavelengths in three spatial directions and 100 periods in time) and wide-angle propagation. Current methods are either based on approximations that favor a specific propagation direction or that require prohibitively large grids. This paper presents the Iterative Nonlinear Contrast Source (INCS) method, which meets all above requirements and provides a full-wave solution of the Westervelt equation. This method treats the nonlinear term from the Westervelt equation as a distributed contrast source. The field is iteratively updated by convolution of an estimate of this nonlinear contrast source with the Green's function of the linear wave equation.

## Iterative solution

In the absence of noticeable attenuation, the behaviour of nonlinear acoustic waves in a homogeneous medium may be described by the lossless Westervelt equation [1]

$$c_0^{-2} \partial_t^2 p - \nabla^2 p = S + \frac{\beta}{\rho_0 c_0^4} \partial_t^2 p^2, \quad (1)$$

in which  $p$  [Pa] is the acoustic pressure,  $\rho_0$  [kg m<sup>-3</sup>] is the ambient density,  $c_0$  [m s<sup>-1</sup>] is the small-signal sound speed,  $\beta$  is the coefficient of nonlinearity, and  $S$  [N m<sup>-4</sup>] represents the action of the primary source. The latter quantity may be written as  $S = \rho_0 \partial_t q - \nabla \cdot \mathbf{f}$ , where  $q$  [s<sup>-1</sup>] denotes the volume density of volume injection rate and  $\mathbf{f}$  [N m<sup>-3</sup>] denotes the volume density of force. The lossless Westervelt equation forms a good description of diagnostic ultrasound propagating in water. However, in human tissue the losses cannot be neglected and it is necessary to include a power-law type of attenuation [2]. The introduction of attenuation may be achieved in a general way by changing Eq. (1) into [3]

$$c_0^{-2} \partial_t^2 [\chi(t) *_t p] - \nabla^2 p = S + \frac{\beta}{\rho_0 c_0^4} \partial_t^2 p^2, \quad (2)$$

where  $\chi(t)$  [m s<sup>-1</sup>] is a normalized compressibility relaxation function and  $*_t$  indicates a temporal convolution.

Both terms at the right-hand side of Eq. (2) may be considered as separate sources that generate their own fields in a background medium. This is the medium that appears in the wave operator at the left-hand side, i.e. a homogeneous medium that is characterized by  $c_0$ ,  $\rho_0$ , and  $\chi(t)$ . In diagnostic nonlinear ultrasound, the second term on the right hand side of Eq. (2) usually has a minor effect on the total field. This nonlinear term will be considered as a nonlinear contrast source

$$S^N(p) = \frac{\beta}{\rho_0 c_0} \partial_t^2 p^2 \quad (3)$$

that provides a small correction  $\delta p(\mathbf{x}, t)$  to the linear field  $p^{(0)}(\mathbf{x}, t)$  that is generated in the background medium by the primary source  $S$ . Now it is supposed that the solution  $G(\mathbf{x}, t)$  of

$$c_0^{-2} \partial_t^2 [\chi(t) *_t G] - \nabla^2 G = \delta(\mathbf{x}) \delta(t) \quad (4)$$

is known. This is the Green's function of the background medium, so the linear field due to  $S$  is

$$p^{(0)} = G *_x *_t S, \quad (5)$$

where  $*_{\mathbf{x},t}$  indicates a convolution over three-dimensional space and time. The field  $p^{(0)}$  may be considered as a zero-order approximation of the total field. This zero-order approximation is used to compute a first estimate  $S^{(1)} = S^N(p^{(0)})$  of the contrast source. Subsequent convolution of  $G$  and  $[S + S^{(1)}]$  yields a first-order estimate  $p^{(1)}(\mathbf{x}, t)$  of the field. With the INCS method, this idea is repeated to obtain successive approximations  $p^{(j)}(\mathbf{x}, t)$  to the total field  $p(\mathbf{x}, t)$  according to [4]

$$p^{(j)} = p^{(0)} + G *_x *_t S^{(j)}, \quad S^{(j)} = S^N(p^{(j-1)}), \quad j=1, 2, \dots \quad (6)$$

In mathematics, this procedure is known as a Neumann iteration. Note that each iteration step in fact involves the solution of the linear field problem for the estimated contrast source in the background medium. Each step requires the spatiotemporal convolution of the contrast source with the background Green's function  $G(\mathbf{x}, t)$

$$p^{(j)}(\mathbf{x}, t) = \int_{\mathcal{D}_T^{(j)}} \int_{\mathcal{D}_X^{(j)}} G(\mathbf{x} - \mathbf{x}', t - t') S^{(j)}(\mathbf{x}', t') d\mathbf{x}' dt'. \quad (7)$$

Here  $\mathcal{D}_T^{(j)}$  and  $\mathcal{D}_X^{(j)}$  denote the spatial and temporal support of estimate  $S^{(j)}$  of the contrast source.

## Discretization

The numerical evaluation of the four-dimensional convolution integral in Eq. (7) forms the most involving

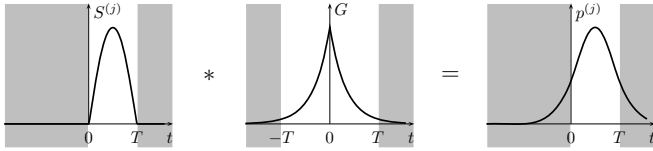


**Figure 1:** The continuous version of the windowing process. If the given support of  $S^{(j)}(t)$  is  $[0, T]$  and the desired domain of interest of  $p^{(j)}(t)$  is also  $[0, T]$ , then the support of  $G(t)$  may be restricted to the domain  $[-T, T]$  without consequences for  $p^{(j)}(t)$  on the desired domain.

operation of the INCS method, both in terms of the computation time and the memory demand. To minimize both aspects, the Fast Convolution (FC) method [4, 5] is employed. In the next subsections, this method will be outlined.

### Simple discretization

A straightforward approach to numerically perform the convolution in Eq. (7) is to use the left Riemann sum with spatial and temporal sampling intervals  $\Delta x$  and  $\Delta t$ , and to approximate the convolution integral by the corresponding four-dimensional convolution sum. For ease of explanation, in this subsection the one-dimensional convolution sum

$$p_n^{(j)} = G_n *_{n} S_n^{(j)} = \Delta t \sum_m G_{n-m} S_m^{(j)}. \quad (8)$$

will be considered instead. Here,  $G_n = G(n\Delta t)$  and  $S_n = S(n\Delta t)$ , while  $p_n^{(j)} \approx p^{(j)}(t)$  at the sampling points  $n\Delta t$ . To end up with a finite number of samples, both  $n - m$  and  $n$  must remain finite, which implies the subjection of  $G(t)$ ,  $S^{(j)}(t)$ , and, consequently,  $p^{(j)}(t)$  to an ideal window. Figure 1 shows the continuous version of this process. In the discrete case, the process is essentially identical. For efficiency, the convolution sum is usually evaluated by applying FFT's. Since this implies a circular convolution, wraparound must be avoided *a priori* by zero-padding. This process is depicted in Fig. 2. Due to the use of FFT's, the computational effort required for the convolution sum is of the order  $2N \log(2N)$ , where  $N$  is the number of grid points before zero-padding. The remaining approximation error  $p_n^{(j)} - p^{(j)}(n\Delta t)$  is due to the sampling and windowing operations. When no prior measures are taken, an accurate evaluation  $p^{(j)}(t)$  may easily involve 10 or more samples per period of the highest significant frequency component in  $S^{(j)}(t)$ . This may result in a prohibitively large amount of grid points, especially for convolutions in more dimensions as considered in this paper. To avoid this problem, the applied FC method employs a more advanced way of discretizing the convolution integral, as will be explained next.

### Advanced discretization

This subsection describes the procedure to obtain a coarse discretization while keeping the approximation error under control. Again, the one-dimensional case is considered for simplicity. The key to attaining a coarse discretization is to avoid the aliasing effect that is described in Fig. 3. This is achieved by filtering all

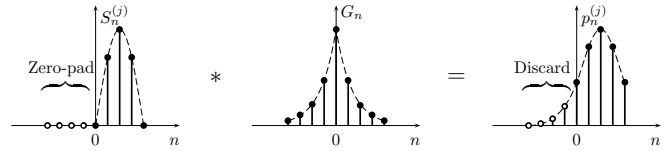


**Figure 2:** The zeropadding process. The support of  $S_n^{(j)}$  and the desired interval of interest of  $p_n^{(j)}$  are both  $[0, N]$ . Supplementing  $S_n^{(j)}$  with zero-valued samples  $S_{-N+1}^{(j)}$  to  $S_{-1}^{(j)}$  avoids wraparound due to circular convolution. The samples  $p_{-N+1}^{(j)}$  to  $p_{-1}^{(j)}$  should be discarded.

relevant functions prior to discretization. The underlying assumption of the FC method is that a maximum angular frequency of interest  $\Phi$  can be chosen in such a way that all components of interest in  $p^{(j)}(t)$  have an angular frequency  $|\omega| \leq \Phi$ . This implies that filtering of  $G(t)$  and  $S^{(j)}(t)$  with an ideal low-pass filter with an angular cutoff frequency  $\Omega \geq \Phi$  only removes insignificant components of  $p^{(j)}(t)$ . By subsequently taking a sampling interval  $\Delta t = \pi/\Omega$ , i.e. sampling at two points per period of  $\Omega$ , the situation  $\Omega = \Omega_{\text{nyq}}$  is enforced and aliasing is avoided. This means that  $p_n^{(j)}$  is obtained as the exact value of the filtered version of  $p^{(j)}(t)$  at the sampling points  $n\Delta t$ . In other words, the approximation error is entirely due to the difference between the filtered and the unfiltered versions of  $p^{(j)}(t)$ , which manifests itself only in the part of the spectrum that is of no interest as long as  $\Omega \geq \Phi$ . With the proposed method, preference is thus given to discarding the contributions from the frequencies  $|\omega| > \Omega$  over making an aliasing error in the frequency range  $|\omega| \leq \Omega$ .

To summarize, the FC method for the coarse discretization of a one-dimensional convolution integral involves:

1. Subjecting  $G(t)$  and  $S(t)$  to an ideal low-pass filter with an angular cutoff frequency  $\Omega \geq \Phi$ , and to a time window with a size  $2T = (2N - 1)\pi/\Omega$ .
2. Sampling  $G^{\Omega, T}(t)$  and  $S^{\Omega, T}(t)$  at  $2N$  points with a sampling interval  $\Delta t = \pi/\Omega$ .

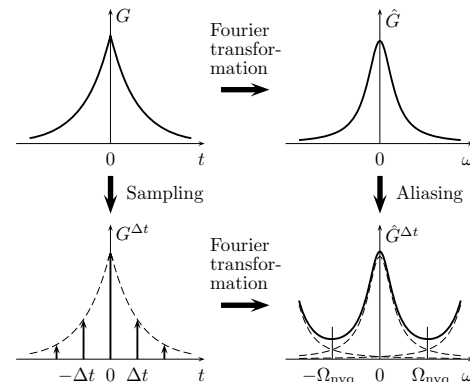


**Figure 3:** The aliasing effect. A function  $f$  (upper left panel) is sampled with a sampling interval  $\Delta t$  (lower left panel). If  $f$  has a spectrum  $\hat{f}$  (upper right panel) that is nonzero for  $|\omega| > \pi/\Delta t = \Omega_{\text{nyq}}$ , then the spectrum of the sampled function differs from the spectrum of the unsampled function on  $[-\Omega_{\text{nyq}}, \Omega_{\text{nyq}}]$ .

3. Obtaining the Fourier transforms of  $G_n$  and the zero-padded  $S_n$  using a  $2N$ -point FFT.
4. Multiplying the Fourier transforms and return to the original domain using a  $2N$ -point inverse FFT.

For the numerical evaluation of the four-dimensional convolution integral in Eq. (7), the method above is applied to all four coordinates of both  $G(\mathbf{x}, t)$  and  $S^{(j)}(\mathbf{x}, t)$ . The temporal angular cutoff frequency  $\Omega$  is taken as the prime parameter for both the temporal and the spatial discretization. This quantity directly determines the temporal sampling interval  $\Delta t = \pi/\Omega$ . Further, it is assumed sufficient to only retain those wave components with real angular wavevectors  $\mathbf{k}$  that satisfy  $|\mathbf{k}| = (k_x^2 + k_y^2 + k_z^2)^{1/2} \leq \Omega/c_0$ . Consequently, in each spatial dimension the maximum possible wavenumber is  $K = \Omega/c_0$  and the resulting spatial sampling interval is  $\Delta x = \pi/K = \pi c_0/\Omega$ .

The spatially filtered and temporally windowed version  $\hat{G}_K^T(\mathbf{x}, \omega)$  of the Green's function may be obtained analytically. For  $\|\mathbf{x}\| \neq 0$  it is obtained as [3, 4]

$$\begin{aligned} \hat{G}_K^T(\mathbf{x}, \omega) = & \frac{\exp(-jk_\alpha\|\mathbf{x}\|)}{4\pi\|\mathbf{x}\|} H(c_0T - \|\mathbf{x}\|) \\ & - \frac{\exp(jK\|\mathbf{x}\|)}{8\pi^2j\|\mathbf{x}\|} \{E_1[-j(K - k_\alpha)\|\mathbf{x}\|] \\ & + E_1[-j(K + k_\alpha)\|\mathbf{x}\|]\} \\ & + \frac{\exp(-jK\|\mathbf{x}\|)}{8\pi^2j\|\mathbf{x}\|} \{E_1[j(K - k_\alpha)\|\mathbf{x}\|] \\ & + E_1[j(K + k_\alpha)\|\mathbf{x}\|]\}, \quad (9) \end{aligned}$$

where  $E_1(z) = \exp(z)E_1(z)$  involves the exponential integral  $E_1(z)$ , and  $H$  is the Heaviside step function. For  $\|\mathbf{x}\| = 0$  the function  $\hat{G}_K^T(\mathbf{x}, \omega)$  is given by

$$\hat{G}_K^T(\mathbf{x}, \omega) = \frac{-jk_\alpha}{4\pi} + \frac{k_\alpha}{4\pi^2} \ln\left(\frac{K - k_\alpha}{K + k_\alpha}\right) + \frac{K}{2\pi^2}. \quad (10)$$

In Eqs. (9) and (10),  $k_\alpha = (\omega/c_0)\hat{\chi}^{1/2}(\omega)$ , where  $\hat{\chi}(\omega)$  is the Fourier transform of the compliance relaxation function  $\chi(t)$ . In the considered domain, the subsequent spatial windowing and temporal filtering are straightforward multiplications with the relevant rectangular windows.

## Numerical results

The INCS method has been implemented in Fortran for evaluation on a SGI Altix 3700 clustered multiprocessor system with Itanium 2 processors running at 1.3 GHz and with 2 GB memory per processor. Currently, four-dimensional spatiotemporal grids with up to  $10^9$  grid points can be dealt with. This corresponds to problems that measure 100 wavelengths in each of the three spatial directions, and 100 periods in time, at the selected maximum frequency of interest. In the next subsections, two sets of results will be presented.

### Directional independence

To assess the directional independence of the INCS method, the nonlinear field of a point source in a

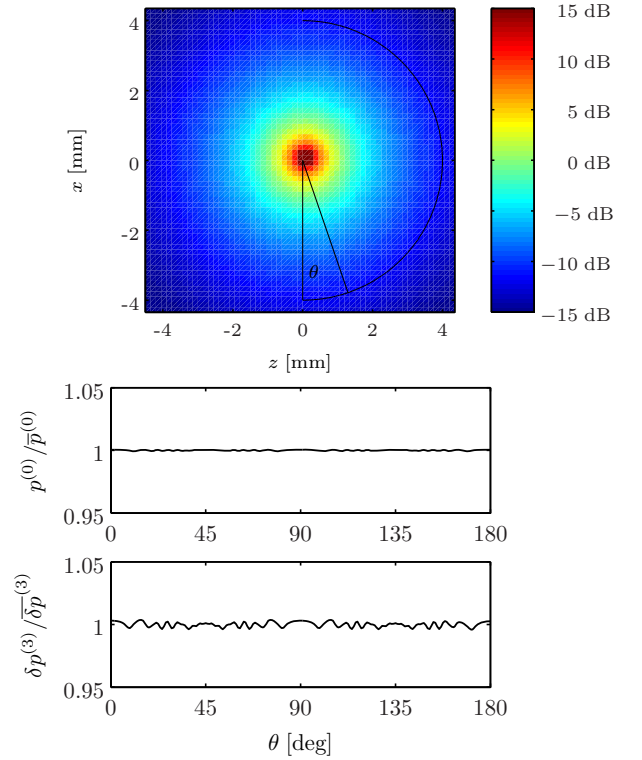


**Figure 4:** Computed pressure field for a point source at the origin, in water. *Top:* The profile of the linear field  $p^{(0)}$  in the plane  $y = 0$ . The 0 dB level corresponds to 500 kPa. *Middle:* The profile of the linear field  $p^{(0)}$  on the semi-circle indicated in the top panel, relative to its mean value  $\bar{p}^{(0)}$  over the circle. *Bottom:* The profile of the nonlinear field correction  $\delta p^{(3)}$  on the semi-circle indicated in the top panel, relative to its mean value  $\bar{\delta p}^{(3)}$  over the semi-circle.

homogeneous domain is evaluated. The employed source is described by

$$S = S_0 S(t) \delta(\mathbf{x}), \quad (11)$$

where  $S_0 = 2\pi \times 10^3 \text{ N m}^{-1}$ , the signature  $S(t)$  is a modulated harmonic signal with a frequency  $f_0 = 1 \text{ MHz}$  and a unit amplitude Gaussian envelope of width  $3/f_0$  between its  $e^{-1}$  values, and  $\delta$  denotes the Dirac delta distribution. In the linear case, i.e. for  $p^{(0)}$ , this results in a pressure of 500 kPa at a distance 1 mm from the source. The medium is water ( $c_0 = 1500 \text{ m s}^{-1}$ ,  $\rho_0 = 1000 \text{ kg m}^{-3}$ ,  $\beta = 3.5$ , no attenuation). The nonlinear pressure field is computed for a domain of  $8.6 \text{ mm} \times 8.6 \text{ mm} \times 8.6 \text{ mm}$  centered at the source, and for a time interval of  $12 \mu\text{s}$ . At the maximum frequency of interest  $F = 5 \text{ MHz}$ , the discretization is  $D_F = 2$ . The Neumann scheme is iterated up till  $j = 3$ .

Figure 4 shows the computed profiles of the pressure field. The top panel shows that the linear field  $p^{(0)}$  has the same decay in all directions. The panels at the middle and the bottom show that the relative deviations in the fundamental and in the third iteration of the nonlinear field correction  $\delta p^{(3)}$  are less than 0.6%, which corresponds to 0.05 dB. From this it may be concluded that the INCS method has the same accuracy in all propagation directions.

## Strongly steered beam

To show that the INCS method can deal with a strongly steered beam, the nonlinear field of a phased array transducer is computed. This source is located in the plane  $z = 0$ , and consists of 48 elements with a width of 0.21 mm, a height of 12 mm, and a pitch of 0.5 mm. The elements are excited with a modulated harmonic signal with a frequency  $f_0 = 1$  MHz and a Gaussian envelope with a width of  $3/f_0$ . The amplitude of the pressure at the surface of the elements is 250 kPa, and the phase steering is such that the generated beam makes an angle of  $45^\circ$  with the  $z$ -axis. The beam is focused at  $(x_f, z_f) = (40 \text{ mm}, 40 \text{ mm})$ . The medium is water. The nonlinear pressure field is computed for a skew domain of  $30 \text{ mm} \times 18 \text{ mm} \times 53 \text{ mm}$  that is located around the beam axis, and for a co-moving time interval of  $36 \mu\text{s}$ . At the maximum frequency of interest  $F = 4$  MHz, the discretization is  $D_F = 2$ . The Neumann scheme is iterated up till  $j = 4$ .

The computed profiles of the fundamental, the second harmonic, and the third harmonic are shown in Fig. 5. The parallelogram-shaped computational domain can clearly be distinguished. The accuracy of the results cannot be tested by a direct comparison with a benchmarking method since all known methods can only deal with strongly steered, nonlinear fields in an approximate way. However, for the case of an unsteered beam [4] an excellent agreement is found between the results obtained by the INCS method and the AS-NLP method [6]. This, together with the observed directional independence, leads to the conclusion that the INCS method provides accurate results for strongly steered beams.

## Acknowledgements

This research was supported by the Dutch Technology Foundation (STW) and the Dutch National Computing Facilities Foundation (NCF).

## References

- [1] M.F. Hamilton and D.T. Blackstock (eds.), *Nonlinear Acoustics*, Academic Press, San Diego, 1998.
- [2] F.A. Duck, *Physical properties of tissue*, Academic Press, London, 1990.
- [3] J. Huijssen, M.D. Verweij and N. de Jong, "Green's function method for modeling nonlinear three-dimensional pulsed acoustic fields in diagnostic ultrasound including tissue-like attenuation," in: Proc. IEEE UFFC 2008 Symposium, pp. 375-378, 2008.
- [4] J. Huijssen, "Modeling of nonlinear medical diagnostic ultrasound," Ph.D. thesis, Delft University of Technology, 2008. URL: <http://repository.tudelft.nl>
- [5] M.D. Verweij and J. Huijssen, "A filtered convolution method for the computation of acoustic wave fields in very large spatiotemporal domains," J. Acoust. Soc. Am. (in press), 2009.

- [6] R.J. Zemp, J. Tavakkoli and R.S.C. Cobbold, "Modeling of nonlinear ultrasound propagation in tissue from array transducers," J. Acoust. Soc. Am. **113**, pp. 139-152, 2003.

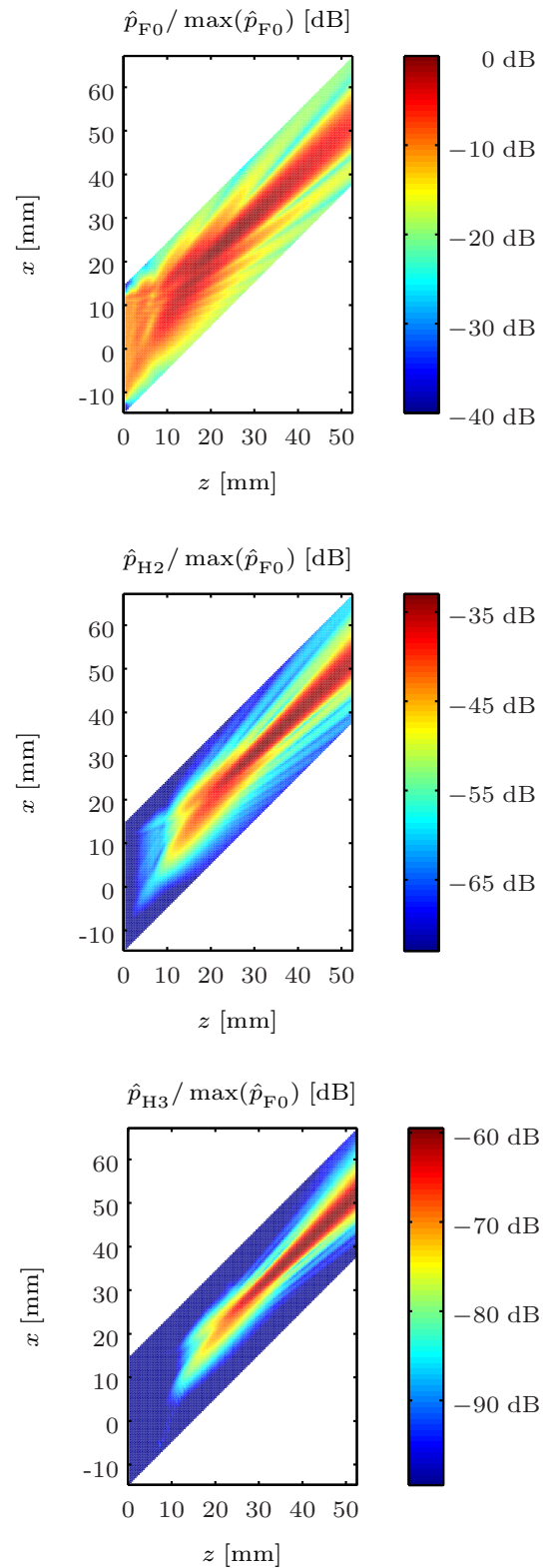


**Figure 5:** Computed pressure field for a phased array steered under  $45^\circ$ , in water. *Top:* The profile of the fundamental. *Middle:* The profile of the second harmonic. *Bottom:* The profile of the third harmonic. All profiles are plotted in the plane  $y = 0$ . The 0 dB level corresponds to 358 kPa.